International Journal of Mechanical, Industrial and Aerospace Sciences
ISSN: 2517-9950
Vol:5, No:9, 2011

DNS of a Laminar Separation Bubble

N. K. Singh and S. Sarkar

***Abstract*—**Direct numerical simulation (DNS) is used to study the evolution of a boundary layer that was laminar initially followed by separation and then reattachment owing to generation of turbulence. This creates a closed region of recirculation, known as the laminar-separation bubble. The present simulation emulates the flow environment encountered in a modern LP turbine blade, where a laminar separation bubble may occur on the suction surface. The unsteady, incompressible three-dimensional (3-D) Navier-Stokes (N-S) equations have been solved over a flat plate in the Cartesian coordinates. The adverse pressure gradient, which causes the flow to separate, is created by a boundary condition. The separated shear layer undergoes transition through appearance of Λ vortices, stretching of these create longitudinal streaks. Breakdown of the streaks into small and irregular structures makes the flow turbulent downstream.

***Keywords*—**Adverse pressure gradient, Direct numerical simulation, laminar separation bubble.

I. Introduction

WHEN a flow at relatively low Reynolds Number encounters an adverse pressure gradient, it may separate from the solid surface. The boundary layer leaves the surface approximately in a tangential direction forming a wedge shaped separated region. The separated but still laminar flow is highly sensitive to external disturbances, which cause the flow to undergo transition. The transition region is located at the outer boundary of the separated shear layer; the thickness of the shear layer grows rapidly and it may finally touch the solid surface as a turbulent layer. The point where the laminar boundary layer separates from the solid surface is known as the *point of separation* and the point where the turbulent boundary layer touches the surface again is known as *reattachment point*. The volume occupied by the regions of separated laminar flow and the turbulent flow is known as *laminar separation bubble.* The structure of a time averaged laminar separation bubble, given by Horton [1] is reproduced in Fig. 1.

The existence of a laminar separation bubble was first recognized by Jones [2]. The work was further carried out by Gault [3]. The most notable advancement in the understanding of bubble structure and behavior came with the work of Gaster [4]. He investigated a large number of bubbles produced on a flat surface.

N. K. Singh is with the Mechanical Engineering Department National Institute of Technology, Kurukshetra, 136119 India (phone: +919671200887; fax: +91-1744-238050; e-mail: kant.nirmal@ gmail.com).

S. Sarkar is with the Mechanical Engineering Department, Indian Institute of Technology , Kanpur, 208016 India, (e-mail: subra@iitk.ac.in).

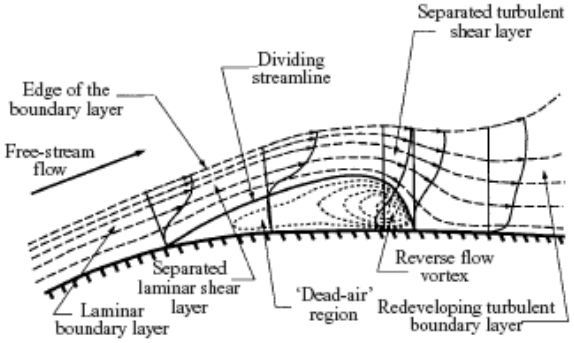

Fig. 1 Structure of a laminar separation bubble

A numerical study of 2-D laminar separation bubble using N-S equations was done by Briley [5]. Pauley and co-workers [6,7] first pointed out the unsteady nature of laminar separation. Pauley's analyses were 2-D and the effects of small-scale turbulence were completely neglected. Alam and Sandham [8] performed a direct numerical simulation (DNS) of the incompressible N-S equations to study flows where laminar boundary-layer separation is followed by turbulent reattachment. Sarkar and Voke [9] studied in detail the physical mechanism of transition of an inflectional boundary layer over the suction surface of a highly cambered low-pressure turbine blade under the influence of periodically passing wakes.

The principal objective of this work is to investigate numerically the flow physics of a laminar separated layer. A laminar separation bubble over a flat plate is created by suction on the upper boundary that produces an adverse pressure gradient. The 3-D unsteady N-S equations for incompressible flow in the Cartesian coordinate have been solved using direct numerical simulation (DNS). Focus is on exploring the mechanism of transition over the laminar separation bubble, flow structures and turbulent statistics near and after the reattachment of the flow.

II. Method

A. Computational domain and grid

The Schematic view of the computational domain is shown in the Fig. 2. The length scales are normalized with respect to inlet boundary layer displacement thickness (δ^*_{in}), and the velocity scale with respect to inlet free stream velocity (U_∞). The box length and the number of grid points used for the simulation are shown in the tabular form in the Table 1.

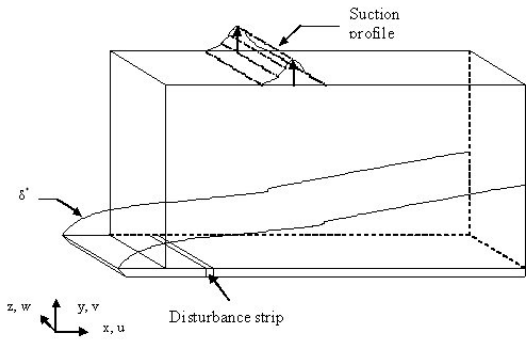

Fig. 2 Schematic drawing of the computational domain

TABLE I
COMPUTATIONAL GRID AND BOX SIZES

Grid points	$L_x(\delta^*_{in})$	$L_y(\delta^*_{in})$	$L_z(\delta^*_{in})$
272×128×128	200	10	30

A uniform grid spacing is used in the streamwise (x) and spanwise (z) directions, whereas, a slow stretching is used in the wall normal direction. A grid-independence test was carried out using four levels of mesh, namely, 200×64×64, 304×80×128, 272×128×128 and 356×128×128 grid points in the x, y and z directions. Variation of mean skin friction coefficient (C_f) for different grids is depicted in Fig 3, while profiles of mean streamwise velocity along with the turbulent kinetic energy (TKE) are shown in Fig 4. It can be seen from Fig.3 that bubble length does not change significantly on further refinement of grid from 272×128×128. Figure 5 further corroborates this fact. It shows that values of mean streamwise velocity change little on further refinement but TKE values do change a bit. Hence, a grid of 272×128×128 points is chosen for the calculations. The near wall resolution at x = 170, where an attached turbulent layer appears, is Δx^+ = 17.5, Δy^+ = 0.59 and Δz^+ = 5.59. Here, the Reynolds number based on δ^*_{in} and U_∞ ($Re_{\delta^*_{in}}$) is 500.

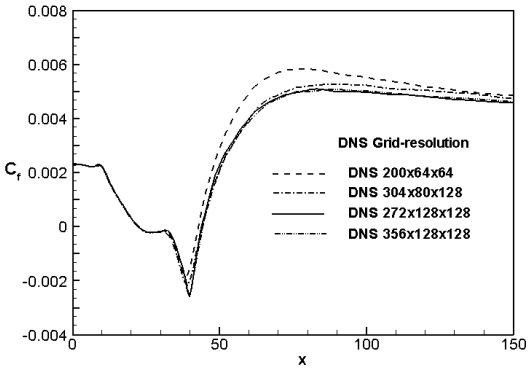

Fig. 3 Grid-resolution test

B. Initial and boundary conditions

The flow field is initiated by specifying a Blasius velocity

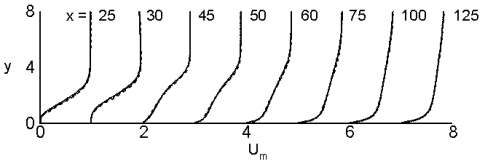

Fig. 4 (a) Profiles of mean streamwise velocity

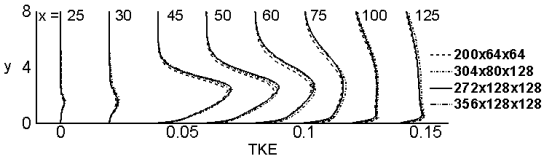

Fig. 4 (b) Profiles of TKE

to the streamwise velocity component and the wall normal velocity is set to zero. At the outlet, a convective boundary condition has been used. In the lower boundary i.e. in the solid wall a no-slip condition is applied. In the present simulation, a disturbance strip is provided at the wall and upstream of separation to trigger the transition. The disturbance is specified by a function to the normal velocity following the work of Alam and Sandham [8].

$$v'(x, z, t) = a_f \exp[-b_f (x-c_f)^2] \sin(\omega t) \sin(\beta z)$$

where, the constant a_f, b_f, and c_f control the streamwise variation of the perturbation. ω is the frequency of the disturbance and β, the span wise wave number. The basic parameters for the disturbance strip are given in the Table II.The simulation is performed on a flat plate and thus an adverse pressure gradient is created by a suitable upper boundary condition for flow to separate. The normal velocity component at the upper boundary has been specified by a Gaussian suction profile by the following expression,

TABLE II
PARAMETERS FOR THE DISTURBANCE STRIP

a_f	b_f	c_f	ω	β
30.08^{-3}	0.125	10	0.15	0.41

$$S(x) = a_s \exp[-b_s (x-c_s)^2]$$

where, the constants a_s, b_s, and c_s control the size, shape and location of the suction profile. The values of the constants are given in the Table 3. A periodic boundary condition is applied to the homogeneous spanwise direction.

TABLE III
PARAMETERS FOR SUCTION PROFILE

a_s	b_s	c_s
0.15	0.02	25

C. Numerical Procedure

In the present simulation the momentum advancement is explicit using the second-order Adams-Bashforth scheme except for the pressure term which is solved by a standard

Projection method. Pressure Poisson equation is discrete Fourier transformed in one dimension (in which periodicity of the flow and so uniformity of the geometry is imposed) and solved using the Bi-Conjugate Gradient method. The spatial discretization is second-order accurate using a symmetry preserving central difference scheme.

The boundary-layer is allowed to grow over the flat plate with imposed boundary conditions. Solution is advanced with a time step of Δt = 0.02 in non-dimensional units that needs 10000 iterations for a flow pass. We allowed seven flow passes with wall disturbances to develop the turbulences and the separation bubble. Statistics were taken for further ten flow passes. All data generated are analyzed by time-averaging as well as through the study of instantaneous dynamics and spectral analysis.

III. Results And Discussion

The aim of the paper, as mentioned earlier, is to study the characteristics of laminar separation bubble subjected to wall disturbances through DNS. Results obtained are compared with the data available in the literature.

A. Mean Skin Friction Coefficient

Figure 4 shows the variation of mean skin friction coefficient for our DNS and compared with the DNS of Alam and Sandham [8]. The potential flow is locally distorted in the vicinity of the bubble that does not allow having a unique value of free-stream velocity. Here the skin friction coefficient is normalized by a local free-stream velocity (U_e) that was defined by integration of spanwise vorticity following Spalart & Strelets [10]

$$U_e(x,y) = -\int_0^y \omega_z dy$$

The plot of the mean skin friction gives information about the mean bubble length. The separation and reattachment points of the mean flow are located by the zero crossing of the skin friction plots.

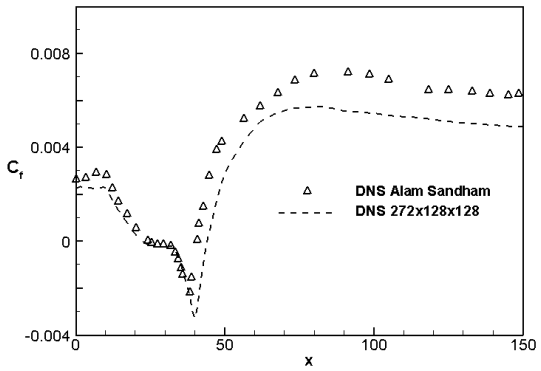

Fig. 5 Comparison of mean skin friction coefficient

In the skin friction distribution, the initial flat portion after the separation point corresponds to the dead air region of the bubble, whereas, the reverse flow vortex region is associated with a much larger negative skin friction. When compared with the corresponding data of Alam and Sandham [8], it is evident that results from present DNS match well their DNS.

B. Mean Flow Structure

A few important variables which are used to describe the mean flow features are Reynolds numbers based on the boundary layer momentum thickness at separation (Re_{θ_s}) and transition length (Re_{lt}). The length of transition is taken here as the distance from separation point to the point of minimum skin friction. The length of separation bubble is also calculated from C_f distributions. The values of the other parameters have been given in the Table 4 and compared with the corresponding values obtained from the DNS [8].

The momentum thickness at separation θ_S and Re_{θ_s} predicted by the present DNS compare well with their results, but the bubble length and Re_{lt} are overpredicted. Figure 6 shows the streamwise velocity contours illustrating the shape of the bubble. The dead-air region and the reverse flow vortex are also indicated. The pictorial views of the bubbles from our DNS and that of Alam and Sandham are almost the same.

TABLE IV
MEAN BUBBLE PARAMETERS

Case	Re_{θ_s}	l_b/δ^*_{in}	θ_s/δ^*_{in}	Re_{lt}
DNS Alam & Sandham	246	-	0.49	6667
Present DNS	205	21.8	0.41	8823

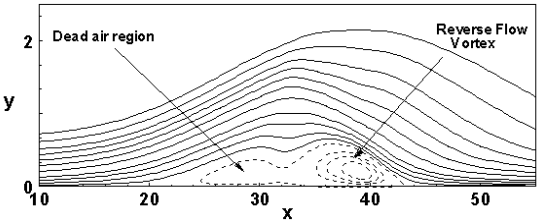

Fig.6 Mean streamwise velocity contours of the laminar separation bubble

Figure 7 shows the mean streamwise velocity component, the r.m.s of streamwise, wall-normal and spanwise velocity fluctuations. The horizontal axis of the Fig. 7 is arbitrarily chosen to represent the variation in magnitude of the variables with respect to the change in position along the streamwise direction. The boundary layer over the flat plate develops against an adverse pressure gradient that cause the boundary layer to separate from the solid surface near x =22 which is reflected by an inflectional velocity profile. It also illustrates the growth of the shear layer, separation bubble with a backflow region and the reattachment point near x=43. After the reattachment, the separated shear layer relaxes downstream slowly towards an equilibrium turbulent boundary layer. Figure 7 also indicates the evolution of turbulence after the separation. Though the perturbations start growing just downstream of separation, the initial growth rate particularly for v' is slow and after x =39 the growth rate is appreciable. This location coincides with the location of minimum C_f. Thus it can be inferred that the generation of turbulence occurs mainly in the reverse flow region and not in

the dead air region. After the reattachment, it takes several bubble lengths downstream to develop the near wall turbulent characteristics.

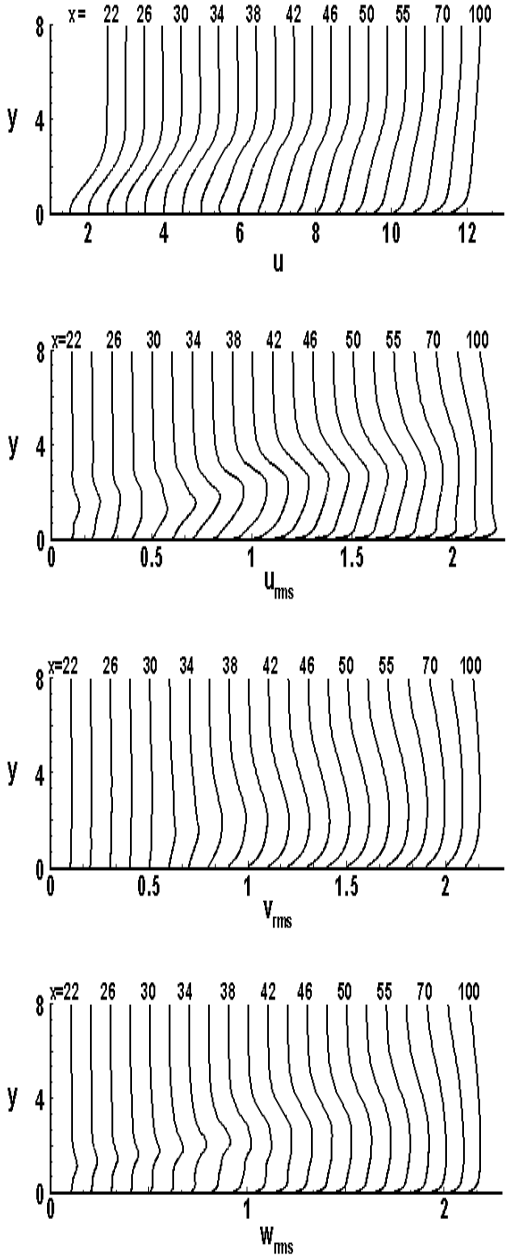

Fig.7 Profiles of mean streamwise velocity, rms streamwise velocity fluctuation, rms wall-normal velocity fluctuation and rms spanwise velocity fluctuation at different locations**.**

C. Instantaneous Flow Field

The instantaneous flow field is very revealing and can be used to explain transition mechanism over the separation bubble, associated flow structures and their breakdown to turbulence after reattachment.Figures 8(a) shows contours of streamwise velocity in *x*-*y* plane (side view) for *z* =30.0. The darkest gray-scale represents the separation region. It also illustrates thickening of shear layer over the bubble and the rollup of shear layer in the outer region illustrating that instability of shear layer occurs via Kelvin-Helmholtz mechanism. This process creates large-scale vortices that may retain their structures far downstream. Thus, near the reattachment, the boundary layer is characterized by predominant outer layer activities that may generate high turbulence in the outer region. Characteristics of near-wall turbulence develop only several bubble lengths downstream.

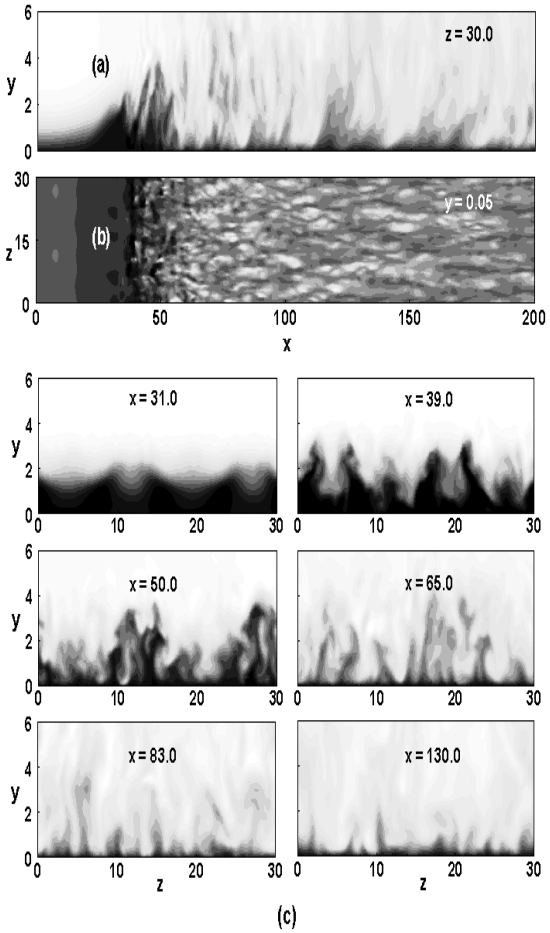

Fig.8 Instantaneous contours of streamwise velocity of a bubble with turbulent reattachment. Maximum level is 0.98, minimum level is -0.13 and the darkest colour shows reversed flow. (a) (x,y)-plane at z = 30.0, (b) (x,z)-plane at y = 0.05, (c) (y,z)- plane at x = 31.0, 39.0, 50.0, 65.0, 83.0 and 131.0.

Figure 8 (b) shows the top view (*x*-*z* plane) of streamwise velocity contours for a wall normal location *y* = 0.05. The top-view illustrates that the initial flow-field is two-dimensional and the boundary separates as laminar. The perturbations appear to grow and the flow ceases to be two-dimensional downstream of *x* = 25. Three-dimensionality appears downstream of *x*=30 and longitudinal streaks, which is the characteristics of transitional layer, appear near *x* =39, This location corresponds to the minimum C_f (Fig.5). The development of these low-speed streaks nears the reattachments regions and their breakdown is also depicted.

Top view further confirms that the near wall turbulence develops far downstream of reattachment

Fig. 8(c) shows the cross-sectional views (y-z plane) of streamwise velocity contours for different streamwise locations at the same time. The contours at x = 31.0 exhibit that the initial symmetry and two-dimensionality is slightly distorted and is completely broken downstream of x = 83.

IV. Conclusions

Direct numerical simulation of a short laminar bubble has been carried out and compared with the data in the literature. The present DNS produces encouraging results, illustrating full transition process over the separation bubble. After the separation, almost no growth of fluctuations is observed in the first 27 percent of bubble length and thereafter the fluctuations increase rapidly. Thus, 3-D motion and non-linear interactions leading to break down to turbulence occur in the second half of the mean bubble length. The simulation also illustrates that the transition process is characterized by break down of longitudinal streaks, which appear via Λ-vortices and vortex stretching mechanism. Turbulence statistics reflects that the turbulent activities are dominant in the outer layer over the rear half of the bubble and near the reattachment. The near wall characteristics develop far downstream indicating a very slow relaxation towards an equilibrium turbulent boundary layer.

References

[1] Horton, H.P., 1968, "Laminar Separation in Two and Three-dimensional Incompressible Flow", PhD Dissertation, University of London.
[2] Jones, B. M., 1934, "Stalling", J. Roy. Aero. Soc., **38**, pp. 753–770.
[3] Gault., D. E., 1957, "A Correlation of Low-speed Airfoil Section Stalling Characteristics with Reynolds Number and Airfoil Geometry", NACA TN 3963.
[4] Gaster, M., 1968, "Growth of Disturbances in Both Space and Time", Phys. Fluids, **11**, pp.723-727.
[5] Briley, W.R., 1971, "Numerical Study of Laminar Separation Bubbles Using the Navier-Stokes Equations", J.Fluid Mech., **47**, Part 4, pp. 713-736.
[6] Pauley, L. L., Moin, P., and Reynolds, W. C., 1990, "The Structure of Two-dimensional Separation", J. Fluid Mech., **220**, pp.397-412.
[7] Ripley M. D., and. Pauley, L. L, 1993, "The Unsteady Structure of Two-dimensional Steady Laminar Separation", Phys. Fluids, *A*, **5**(12).
[8] Alam. M., and Sandham, N. D., 2000, "Direct Numerical Simulation of 'Short' Laminar Separation Bubbles with Turbulent Reattachment", J. Fluid Mech, **403**, pp.223-250.
[9] Sarkar, S., and Voke, P., 2005a, "Large Eddy Simulation of Unsteady Surface Pressure Over a LP Turbine Blade due to Interactions of Passing Waves and Inflexional Boundary Layer", Proceedings of GT 2005 ASME Turbo Expo 2005.
[10] Spalart P.R., and Strelets, M.K.,1997, "Direct and Reynolds-averaged Numerical Simulation of a Transitional Separation Bubble", 11th symp. on Turbulent shear Flows, Grenoble , France.